Termination shock and heliosheath effects on cosmic ray energy changes in the heliosphere

R.A. Caballero-Lopez[a,c], H. Moraal[b,c] and F.B. McDonald[c]

(a) Instituto de Geofísica, UNAM, 04510, México
(b) School of Physics, North-West University, Potchefstroom 2520, South Africa
(c) Institute for Physical Science and Technology, University of Maryland, College Park, MD, 20742, USA
Presenter: R.A. Caballero-Lopez (rogelioc@geofisica.unam.mx), mex-caballero-lopez-RA-abs3-sh33-poster

Adiabatic energy losses form a well-understood part of cosmic ray modulation. However, shock acceleration at the termination shock and the modulation in the heliosheath beyond this shock alter the net cosmic ray energy changes from that in the standard models. This paper compares cosmic ray energy changes in several versions of the modulation process, from the simplest Force-Field model to one with a shock and heliosheath included.

1.   Introduction

The energy loss of cosmic rays in the radially expanding solar wind in the heliosphere is an integral part of the cosmic ray modulation, the other three processes being diffusion, convection and drift in the heliospheric magnetic field (HMF) in the solar wind. In the Force-Field approximation of the theory by [1], all three physical processes are, in fact, combined into a single modulation potential (and consequent energy loss). These energy losses are used for the interpretation of observations, and on the whole are well understood. However, the acceleration and modulation of cosmic rays at the termination shock of the solar wind and in the heliosheath downstream of this shock, has become increasingly important in our understanding of the overall modulation. Specifically, the shock accelerates cosmic rays, while in the divergence-free downstream medium of the heliosheath there are no adiabatic losses. In view of this, we update a set of standard energy loss calculations done by [1], [2] and [3] to estimate the net energy change of galactic cosmic rays in this more realistic model of the heliosphere.

In an accompanying paper we discuss applications of these energy change mechanisms and apply them to the example of K-capture cosmic ray secondaries, where the ratio of these secondaries to their primary progenitors is quite sensitive to energy loss processes, as was shown by [4] and [5].

2.   Calculations

We calculate energy losses in the heliospheric modulation process from numerical solutions of the cosmic ray transport equation for the evolution of the cosmic ray distribution function f in terms of particle momentum, p:

$$\frac{\partial f}{\partial t} + \mathbf{V} \cdot \nabla f - \nabla \cdot (\mathsf{K} \cdot \nabla f) - \frac{1}{3}(\nabla \cdot \mathbf{V})\frac{\partial f}{\partial \ln p} = 0. \tag{1}$$

Here $\mathbf{V}$ is the solar wind velocity and $\mathsf{K}(\mathbf{r}, P, t)$ the diffusion tensor which contains elements $\kappa_\parallel(\mathbf{r}, P, t)$ and $\kappa_\perp(\mathbf{r}, P, t)$ for scattering along and perpendicular to the HMF, B, together with an antisymmetric coefficient $\kappa_T = \beta P/(3B)$ which describes gradient, curvature, neutral sheet, and shock drift effects . The HMF structure is described by the standard Parker spiral magnetic field, given in spherical polar coordinates (r, θ, ϕ) by $\mathbf{B} = B_e(r_e/r)^2(\mathbf{e}_r - \tan\psi\mathbf{e}_\phi)$, with $\tan\psi = \Omega(r - r_0)\sin\theta/V$, where Ω is the angular frequency of solar rotation, and r_0 is the Alfven radius of several solar radii. The values of the field at Earth, B_e, vary from 5 to
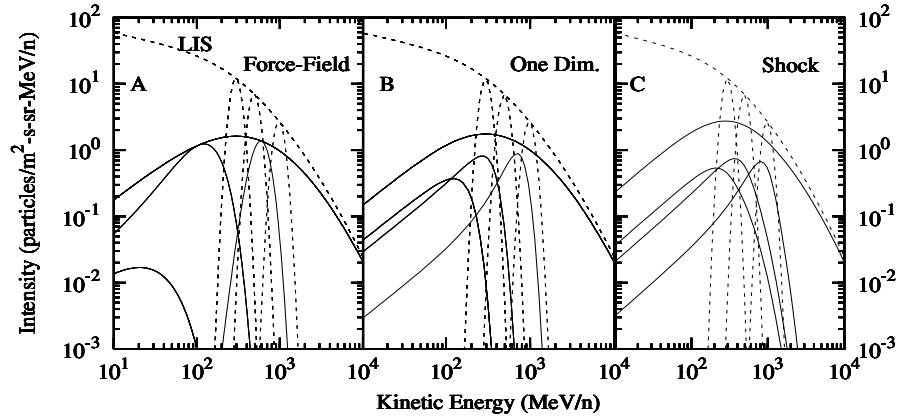
Figure 1. Modulation examples for protons, showing assumed LIS in dashed, and modulated spectra at Earth in full lines. Modulation is shown for full LIS and three Gaussians. (a) Force-Field solution. (b) One-dimensional steady-state solution of the transport equation. (c) Two-dimensional time-dependent shock-heliosheath solution (with no drifts).

10 nT from solar minimum to maximum. The diffusion coefficients can be written in terms of mean free paths by $\kappa = 3\lambda/v$, and the radial and latitudinal components are $\lambda_{rr} = \lambda_\parallel \cos^2 \psi + \lambda_\perp \sin^2 \psi$, $\lambda_{\theta\theta} = \lambda_\perp$.

All energy loss calculations are compared with the widely used Force-Field energy loss. The Force-Field formalism was derived by [6] and [7], recast in its generally used form by [1], and summarized by [8]. It assumes that the radial cosmic ray streaming is zero in a spherically symmetric heliosphere, leading to the result that a particle observed with rigidity P somewhere inside the heliosphere had a rigidity P^* on the outer modulation boundary given by

$$\int_P^{P^*(r,P)} \frac{\beta(P')\kappa_2(P')}{P'} dP' = \int_r^{r_b} \frac{V(r')}{3\kappa_1(r')} dr' \equiv \phi(r), \qquad (2)$$

where κ_{rr} is assumed separable in the form $\kappa_{rr}(r, P) = \beta\kappa_1(r)\kappa_2(P)$. This produces an energy loss $\Delta T = Ze\phi$, where Ze is is the particle charge. The solution of the Force-Field equation then is $f(r, P) = f(r_b, P^*)$, where f is the omnidirectional distribution function, related to the kinetic energy intensity spectrum by $f \propto j_T/P^2$. Values of $\kappa_1(r) = 6\times10^{22}$ cm²/s (independent of r) and $\kappa_2(P) = P$, with P in units of GV, are used here. The outer boundary of the modulation region is put at $r_b = 150$ AU. For $V = 400$ km/s these values give ϕ = 500 MV, which produces an amount of modulation observed roughly between solar minimum and maximum.

3. Results

Calculations were done for protons with an LIS on the outer modulation boundary given by $j_{Tb} = 21.1T^{-2.8}/(1 + 5.85T^{-1.22} + 1.18T^{-2.54})$. Other model details are given by [9]. Figure 1 shows intensity spectra calculated from (a) the Force-Field equation with the parameters above (b) the simple one-dimensional steady-state transport equation of [8] with the same parameters, and (c) the solution of the time-dependent transport equation of [9] which contains a termination shock at 90 AU. This shock has a compression
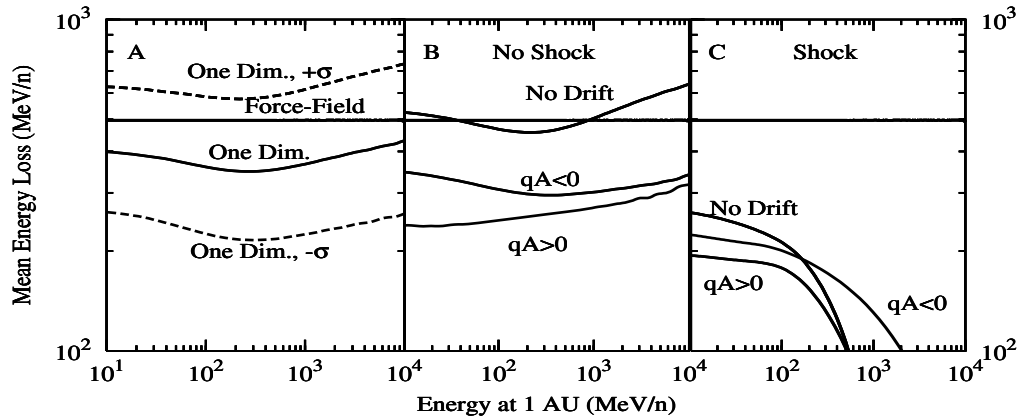
Figure 2. Mean energy losses, $\Delta T =< T^* > -T$, suffered by particles observed at Earth. (a) The Force-Field energy loss compared to that of a one-dimensional steady-state solution of the transport equation with the same parameters. The dashed lines indicate the wide band from within which 68% of the particles orginate in the LIS. (b) The steady-state two-dimensional solution with no shock, for the no-drift and qA>0 and qA<0 drift cases. (c) The same as (b) but for the time-dependent shock-heliosheath solution with a strong shock inserted at r_s = 90 AU.

ratio $s = 4$, and outside the shock the solar wind falls off $\propto r^{-2}$ up to $r_b = 150$ AU. As described in that paper, this means that cosmic rays in the heliosheath do not suffer adiabatic losses. The dashed upper curve in each panel is the LIS, while the full line is the modulated spectrum at Earth. In addition to these full-spectrum solutions, we also show three Gaussian input spectra together with their modulated spectra, in the same format as in [3]. These Gaussians demonstrate the spreading in energy due to energy changes. The modulated peaks for the Force-Field case shift down the furthest, indicating that it gives the largest energy loss. The ones for the one-dimensional steady-state case also have long tails, while the shock/heliosheath solutions show the energy gain due to acceleration by the shock. The qA>0 and qA< 0 drift cases for both the no-shock and shock-heliosheath solutions produce qualitatively similar results and are not shown. Notice that particles with a given energy T^* on the boundary produce particles with a range of energies, T, at the point of observation inside the heliosphere. Conversely, particles observed with energy T at the point of observation have come from a range of energies T^* in the LIS. Average energy losses were calculated by dividing up the LIS in a large amount of Gaussian spectra, and then counting the contribution of each to the intensity at energy T. The average energy in the unmodulated spectrum, $< T^* >$, is then that value above which half the contribution has come. Figure 2 shows the average energy loss $< \Delta T >=< T^* > -T$ as function of kinetic energy T at Earth, for eight different scenarios. The horizontal line is the solution of the Force-Field equation (2) with the parameters stated there, which gives an energy loss of 500 MeV for all energies. All other energy losses are compared to this value. The second solution in Figure 2a is the steady-state one-dimensional solution of (1) with the same parameters. The energy loss is fairly independent of energy, but $\approx 20\%$ smaller than the Force-Field loss, which confirms that the Force-Field overestimates the amount of energy loss, as was pointed out by [8]. The two dashed lines on Figure 2a indicate the spread in energy loss. They define the one-σ limits, i.e. 68% of the particles observed at T have suffered energy losses between these limits. All other solutions have similar energy spreads, and they will therefore not be shown.

Figure 2b shows solutions of the widely applied two-dimensional (radial distance, polar angle) transport equation for no-drift and qA>0 and qA<0 drift states. In this case V and κ_{rr} in the ecliptic plane are the same as for the one-dimensional and Force-Field cases. V increases from 400 to 800 km/s between latitudes 10 and 30 °. κ_{rr} has no latitudinal dependence. Latitudinal diffusion $\kappa_{\theta\theta} = 10\%$ of κ_{rr} is added. In the drift cases a wavy sheet tilt angle of 10° is assumed. These parameters provide a best fit to solar minimum observations (see [9]). The drift solutions have significantly less energy loss than the no-drift, the one-dimensional and the Force-Field solution. The general rule is that as more and easier spatial routes of access are opened up, the less migration there is in energy.

Finally, Figure 2c shows the same cases of Figure 2b, but with a solar wind termination shock ($s = 4$) inserted at r_s= 90 AU. Here κ_{rr}, $\kappa_{\theta\theta}$ and V all drop by a factor of s, and V decreases further $\propto r^{-2}$ in the heliosheath. Since the transport parameters inside the shock are identical to those of Figure 2b, the differences between these two figures are due to the acceleration on the shock and the turn-off of the adiabatic losses in the heliosheath. Once again, the qA>0 and qA<0 solutions offer the best fits to observations inside the shock at solar minimum conditions (see [9]). In this case the energy losses are much less, particularly at high energies where the acceleration at the termination shock reduces the net loss.

All results are shown for protons. Conversion to other species is readily done by noting that two species have the same modulation if they have the same κ, which is $\propto \beta P$. Using the relation $P = pc/q = A/Z\sqrt{T(T+2E_0)} = (A/Z)\beta(T+E_0)$, between momentum p, rigidity, P, kinetic energy per nucleon, T, and speed $\beta = v/c$, where A and Z are mass and charge number, and $E_0 = 938$ MeV, one can transform from one species to another. [10] showed that, while this is complicated for all energies, both the relativistic and non-relativistic limits are that two species have the same κ (i.e. βP) if $[(A/Z)T]_1 = [(A/Z)T]_2$.

4. Conclusions

The two primary conclusions from this analysis are, first, that for a given set of modulation parameters the Force-Field formalism produces up to twice as much energy loss than more realistic no-shock models. Second, the acceleration at the solar wind termination shock is so strong that at high energies it offsets much of the adiabatic losses in the supersonic solar wind. These results have important implications for the interpretation of certain observations, and in an accompanying paper we investigate the example of the modulated secondary to primary ratio in the cosmic ray intensity.

References

[1] L.J. Gleeson and I.A. Urch, Astrophys. Space Sci., 25, 387–404, (1973).
[2] L.J. Gleeson and I.A. Urch, Astrophys. Space Sci., 11, 288–308, (1971).
[3] M.L. Goldstein et al., Phys. Rev. Lett. 25, 832, (1970).
[4] S.M. Niebur et al., *J. G. R.*, 108 (A10), 8033, doi:10.1029/2003JA009876, (2003).
[5] R.A. Mewaldt et al., AIP Conf. Proc. 719, 127-132, (2004).
[6] L.J. Gleeson and W.I. Axford, Can. J. Phys., 46, S937, (1968).
[7] L.J. Gleeson and W.I. Axford, Astrophys. J., 154, 1011, (1968).
[8] R.A. Caballero-Lopez and H. Moraal, J. G. R., 109, A01101, doi:10.1029/2003JA10098, (2004).
[9] R.A. Caballero-Lopez et al., J.G.R., 109, A05105, doi:10.1029/2003JA010358, (2004).
[10] C.D. Steenberg, Ph.D. thesis, Potchefstroom University, (1998).